ELSEVIER

Hearing Research 151 (2001) 79–94

HEARING RESEARCH

www.elsevier.com/locate/heares

Auditory nerve responses to monophasic and biphasic electric stimuli

Charles A. Miller [a,b,*], Barbara K. Robinson [a], Jay T. Rubinstein [a,c], Paul J. Abbas [a,b], Christina L. Runge-Samuelson [b]

[a] *Department of Otolaryngology, Head and Neck Surgery, University of Iowa Hospitals and Clinics, 21201 PFP, 200 Hawkins Drive, Iowa City, IA 52242, USA*

[b] *Department of Speech Pathology and Audiology, University of Iowa, Iowa City, IA 52242, USA*

[c] *Department of Physiology and Biophysics, University of Iowa, Iowa City, IA 52242, USA*

Received 26 July 2000; accepted 5 September 2000

Abstract

Charge-balanced, biphasic stimulus pulses are commonly used in implantable cochlear prostheses as they can be safely delivered to living tissue. However, monophasic stimuli are more efficient (i.e. producing lower thresholds) and likely provide more spatially selective excitation of nerve fibers. We examined the neural responses to monophasic, 'pseudomonophasic', and biphasic stimuli to better understand the inherent tradeoffs of these stimuli. Using guinea pig and cat animal models, we compared the auditory nerve responses to both 40 μs monophasic and 40 μs/phase biphasic stimuli using both electrically evoked compound action potential and single-fiber recordings. We also made comparisons using a computational model of the feline auditory nerve fiber. In all cases, our stimuli were cathodic monophasic and cathodic-first biphasic pulses. As expected, monophasic stimuli provided lower thresholds relative to biphasic stimuli. They also evoked responses with relatively longer latencies. We also examined responses to charge-balanced biphasic pulses composed of two phases of differing duration (i.e. pseudomonophasic stimuli). The first phase was fixed at 40 μs, while the second phase was systematically varied from 40 to 4000 μs. With a relatively long second phase, we hypothesized that these stimuli would provide some of the beneficial features of monophasic stimuli. Both the gross-potential and single-fiber data confirmed this and indicate that the largest incremental effects of changing the second-phase duration occur for durations less than 500 μs. Consideration of single-fiber data and computer simulations suggest that these results are consistent with the neural membrane acting as a leaky integrator. The computer simulations also suggest that the integrative properties at least partially account for the difference between our monophasic–biphasic results and previously published data. Our results apply to cathodic-leading stimuli; due to differing patterns of membrane depolarization, they may not be applicable to situations using anodic-leading stimuli. Finally, we observed differences between the guinea pig and cat response patterns. Compared to cats, guinea pigs produced smaller monophasic vs. biphasic threshold differences. This interspecies disparity may be due to differences in cochlear anatomy.

Key words: Auditory prosthesis; Electric stimulation; Cochlear nerve; Evoked potential; Auditory nerve fiber; Cat; Guinea pig; Monophasic; Biphasic

1. Introduction

Safety considerations dictate that charge-balanced, biphasic stimuli are used for functional electrical stimulation of excitable tissue. However, compared to monophasic stimuli, biphasic pulses are less efficient. Neural membranes integrate externally applied current, so that the second phase of a biphasic stimulus reduces the effective strength of the leading stimulus phase. While monophasic stimuli are contraindicated, a class of biphasic stimuli referred to as 'pseudomonophasic' stimuli have promise of improved efficiency while maintaining charge balance. The goal of our study was to characterize the neurophysiological responses to monophasic, pseudomonophasic, and biphasic stimuli using gross-potential, single-fiber, and computational modeling approaches and determine the relative merits of each stimulus.

* Corresponding author. Tel.: +1 (319) 384-6758; Fax: +1 (319) 353-6739; E-mail: charles-miller@uiowa.edu

0378-5955/01/$ – see front matter
PII: S0300-2977(00)00082-6

1.1. Previous relevant research

Neural thresholds to biphasic, charge-balanced, rectangular current pulses depend strongly on the duration of each phase. The integrative property of neural membranes is well established (e.g. Bostock, 1983) and is reflected in strength–duration data obtained with auditory nerve single-fiber (e.g. van den Honert and Stypulkowski, 1984) and gross-potential (e.g. Abbas and Brown, 1991) techniques, as well through psychophysical measures (e.g. Pfingst et al., 1991). However, compared with biphasic stimuli, monophasic pulses excite neurons at lower thresholds. Using frog sciatic nerve preparations, van den Honert and Mortimer (1979) reported relatively lower monophasic thresholds and described a threshold advantage gained by delaying the second phase of a biphasic pulse relative to the first phase. Measuring psychophysical thresholds from a guinea pig with a cochlear implant, Miller et al. (1995) reported that monophasic thresholds were 4–10 dB lower than biphasic thresholds for phase durations ranging from 20 to 400 μs/phase, respectively. Miller et al. (1999a) compared thresholds obtained from four feline single fibers excited by monophasic and biphasic current pulses. Using 40 μs/phase pulses, they reported threshold reductions with monophasic pulses ranging from 2 to 9 dB, with a mean reduction of 6 dB. They also noted that the threshold difference obtained by reversing stimulus polarity (i.e. from cathodic to anodic) was greater with monophasic pulses than with biphasic pulses. In three of four fibers, there was almost no change in threshold with polarity reversal when biphasic pulses were used. Shepherd and Javel (1999) examined stimulus polarity and waveform effects in a survey of 14 single fibers. Using 100 μs/phase pulses, they observed a mean biphasic/monophasic threshold difference of 1.2 dB. They also noted a negligible (0.2 dB) change in threshold with polarity reversal when biphasic pulses were used. The single-fiber polarity reversal data suggest that, at least for short-duration pulses, current integration occurs across the two phases. This is also consistent with the fact that biphasic thresholds are higher than monophasic thresholds.

The computational modeling work of Frijns et al. (1996) suggests that monophasic stimuli also produce more spatially restricted patterns of neural excitation. McIntyre and Grill (2000) also demonstrated better spatial selectivity with monophasic stimuli in their modeled fibers of the central nervous system. Greater specificity of neural excitation would likely lead to improved performance with cochlear prostheses. However, due to safety concerns regarding the net delivery of charge to living tissue (e.g. Brummer et al., 1983), monophasic pulses are not used in clinical applications. Some studies, however, have examined the use of 'asymmetric' biphasic or triphasic current pulses that could perhaps produce the threshold advantage obtained with monophasic pulses, while maintaining the safety of charge balance. In a psychophysical study of implanted monkeys, Coste and Pfingst (1996) compared behavioral thresholds obtained using biphasic and triphasic stimulus pulses. The latter stimuli consisted of three phases of equal duration, with the middle phase opposite in polarity and twice the amplitude of the first and third phases. This stimulus was designed to simulate a monophasic pulse while maintaining charge balance. However, no threshold decrease was found with the triphasic stimuli in comparison with biphasic stimuli. In their single-fiber study, Shepherd and Javel (1999) compared thresholds to both 100 μs/phase biphasic and 'asymmetric' biphasic stimulus pulses. In data from one fiber, they showed that a threshold reduction was achieved through the use the 'asymmetric' stimulus, in which the second phase was twice as long as the first (i.e. 200 μs vs. 100 μs), but of half the amplitude.

1.2. Goals and approach

We were motivated by three goals. First, we sought to clarify and extend the findings of previously reported studies of differences obtained with biphasic and monophasic stimuli. Our previous single-fiber experiment was based on a small data set and the results differed in magnitude from that of Shepherd and Javel (1999). In contrast to other efforts, we have chosen to present stimuli through a monopolar electrode, providing an arguably better basis for interpreting electrophysiological data since a monopole provides a relatively simple and uniform excitation field compared to that created by a dipole. We also wanted to quantify the range of second-phase durations that have measurable effects on neural response properties. Such data are relevant to efforts seeking to optimize the use of 'pseudomonophasic' stimuli, where the second phase is prolonged to approximate the useful properties of monophasic stimuli. A second goal was to collect single-fiber and gross-potential data from the same subjects and using the same stimulus paradigms. Such data would be useful in providing norms for the development of computational models of the auditory nerve as well as understanding how well single-fiber properties are reflected in the whole-nerve potential. Modeling efforts of Frijns et al. (1996) and Miller et al. (1999b) have shown that the fiber population recruitment pattern influences the gross response of the nerve in ways not predicted from single-fiber responses. Also, with the advent of clinical cochlear implant devices that can record the electrically evoked compound action potential (ECAP), proper interpretation of the ECAP is essential for effective clin-

ical applications. Our third goal concerned across-species comparisons of evoked responses. Both the guinea pig and cat are useful models for cochlear implant research and both have unique advantages. The feline model can be used to probe both single-fiber and gross-potential responses, a particularly critical feature for efforts to produce realistic computational models of the mammalian auditory nerve. The guinea pig is also an attractive animal model, given its relatively modest costs. However, compared to cats and humans, the overall shape of the guinea pig cochlea is somewhat different and may underlie some of the species differences that we have previously reported (Miller et al., 1998). If those differences are indeed attributable to the gross cochlear anatomy of the guinea pig, it could limit, in some cases, the usefulness of extrapolating data from that species to that of humans. We therefore deemed it prudent to investigate response properties in both the cat and guinea pig.

2. Materials and methods

2.1. Surgical preparation

Guinea pigs and cats free from middle-ear infection were used in anesthetized, acute, preparations. ECAP data were obtained from 11 guinea pigs and 13 cats; single-fiber recordings were obtained from 27 units of four cats. Surgical and experimental protocols were approved by the University of Iowa Animal Care Unit and complied with NIH animal use standards.

Guinea pigs were anesthetized with a combination of ketamine (40 mg/kg), xylazine, (7.5 mg/kg), and acepromazine (0.5 mg/kg), administered intramuscularly. Maintenance doses of 33–50% of the initial amount were given as needed. A single dose of atropine sulfate (0.05 mg/kg, s.q.) was also given. A catheter inserted into the external jugular provided a route for hydration (with Ringer's solution) and chemical deafening. A tracheotomy was performed and closed ventilation provided by a Harvard Apparatus model 665 ventilator and pure oxygen (5 ml tidal volume, 50 cycles/s). The head was immobilized with an armature, screws and dental acrylic affixed to the skull. Rectal temperature, heart rate, and blood oxygen level were monitored with a Pace Tech 4000B vital signs monitor. Expired CO_2 partial pressure was monitored with a BCI Industries capnometer and maintained between 20 and 35 mm Hg. Anesthesia level was assessed by heart rate, respiration pattern, and pinch reflex. Core body temperature was maintained at 38.4 ± 1.5°C with a circulating water heating pad and drapes. The auditory nerve was exposed through a posterior fossa approach. The flocculus was exposed and retracted medially with cotton to expose the nerve. A bipolar recording electrode, mounted on a micromanipulator, was lowered into the defect and positioned on the nerve, with the positive electrode in contact with the nerve. The bulla was opened to expose the base of the cochlea. A cochleostomy was drilled at a site posterior to the round window with a 0.6 mm burr. A 0.005″ diameter Pt/Ir wire (bared of insulation to expose a 1 mm length) was inserted into the scala tympani via this defect.

Similar procedures were used for cats. A pre-anesthetic sedative of ketamine (30 mg/kg) and acepromazine (0.3 mg/kg) was administered subcutaneously. Atropine sulfate (0.04 mg/kg/12 h, s.q.) was given to reduce mucosal secretions. The femoral vein was then catheterized and served as a route for a continuous drip of Ringer's solution (2 ml/kg/h) and sodium pentobarbital anesthesia. The initial dose of the barbiturate was 8 mg/kg, followed by smaller doses (2–3 mg/kg) administered to effect. Boli of dexamethasone were administered intravenously (i.v.) (1.0 mg/kg/12 h) to reduce edema. A tracheotomy was performed to provide ventilation with oxygen (25 ml tidal volume at 45–60 cycles/s). As with guinea pigs, anesthesia level and vital signs were continuously monitored. Body temperature was maintained at 38.6 ± 1.5°C using a heating pad and drapes. The head was immobilized with a bite bar. The auditory nerve was exposed using a posterior fossa approach. A head-mounted retractor was used to medialize the cerebellum to expose the auditory nerve near the porus acousticus; cotton provided additional retraction near the nerve. In some cases (C55, 56, and 57), a cochleostomy was performed and a ball electrode inserted into the scala tympani of the basal turn for intracochlear stimulation. However, in the 10 previous cats, the round window was excised to facilitate local infusion of ototoxin. In those subjects, a 0.35 mm diameter Pt/Ir stimulating ball electrode was inserted through the round window defect into the basal turn, as described in Miller et al. (1998).

2.2. Deafening protocols

All guinea pigs were deafened using a systemic application of kanamycin and ethacrynic acid. Following the protocol of West et al. (1973), kanamycin was administered (400 mg/kg, s.q.) 90–120 min prior to injection of ethacrynic acid (40 mg/kg, i.v.) via the external jugular. For three cats (C55, 56, and 57), these same drugs were used, following the protocol of Xu et al. (1993). The effectiveness of this procedure was assessed by monitoring the click-evoked compound action potential or auditory brainstem response at 5 min intervals both before and after administration of the ethacrynic acid. Loss of acoustic sensitivity was confirmed by observing a minimum 60 dB threshold increase of the evoked

response. For all other cats, deafening was accomplished by intracochlear infusion of 100 μl of 10% (w/v) neomycin sulfate dissolved in water, as described in Miller et al. (1998).

2.3. Stimulus presentation

Stimuli were generated by custom software controlling a 12-bit digital-to-analog converter operating at 100 000 samples/s. That, in turn, was connected to a capacitively coupled, optically isolated current source having a 10–90% rise–fall time of 10 μs and an output time constant of 130 ms. The positive output of the current source was connected to the monopolar stimulating electrode in the basal turn of the cochlea and the negative output was connected to a needle electrode placed in the forepaw. All stimuli were rectangular pulses having one or two phases; we identified stimulus polarity by that of the first phase. Stimuli were presented repeatedly to obtain time-averaged recordings. Cathodic and anodic stimulus pulses were presented in an interleaved fashion; the interstimulus interval (the time between onsets of successive cathodic and anodic pulses) was 30 ms. The relatively long time constant of the current source was chosen to provide long-term charge balance and negligible waveform distortion. In the case of monophasic stimuli, it would result in a small deviation from baseline (zero current) of no more than 0.5% of the peak value of the stimulus pulse. A phase duration of 40 μs was always used for monophasic stimuli and the first phase of biphasic stimuli. In the experiments manipulating the second-phase duration of biphasic pulses, the second-phase amplitude was adjusted to assure charge balance. All stimulus levels were measured from the baseline to the peak of the first phase. Example monophasic and biphasic waveforms (with varying second-phase duration) are shown in Fig. 1. To record single-fiber action potentials, a search stimulus was presented at a level sufficient to evoke an ECAP at least 75% of its maximum (saturation) amplitude. After isolating a fiber, each stimulus was presented 100 times in order to obtain firing rate and spike timing statistics. The stimulation rate was the same as that used for ECAP recordings.

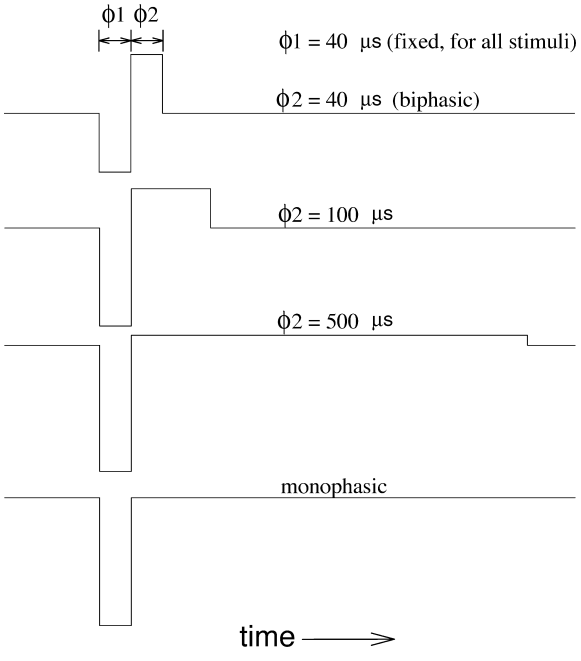

Fig. 1. Idealized examples of biphasic and monophasic stimuli used in this study. In all cases, the first phase was a cathodic, 40 μs rectangular pulse. With biphasic pulses, the first phase was immediately followed by a second, recovery phase. The duration of the second phase was systematically varied and its amplitude adjusted to provide no net charge transfer.

2.4. Recording techniques

Gross neural potentials were recorded with a Pt/Ir ball electrode (0.3–0.4 mm diameter) positioned directly on the nerve trunk. It was connected to the non-inverting input of a custom-built 20 dB differential amplifier. A second ball electrode, oriented 2 mm above the nerve, was connected to the inverting input. Both electrodes were kept bathed in 0.9% saline solution. The amplifier output was low-pass-filtered (sixth order Butterworth, 30 kHz cut-off) and digitally sampled (100 000 samples/s, 16 bits) prior to signal averaging. Each average comprised 100–4000 acquisitions, depending upon observed signal-to-noise conditions, and was digitally stored for later analysis.

Standard micropipette techniques were used to record single-fiber action potentials; details have been described in Miller et al., (1999a). Potentials were amplified (20 or 40 dB gain) and low-pass-filtered (10 kHz cut-off, 40 dB/decade) by an Axon Instruments Axoprobe headstage and amplifier. Additional bandpass filtering (100 Hz Butterworth high-pass, 40 dB/decade; 10 kHz low-pass, 40 dB/decade) was used prior to sampling with 16-bit resolution at 100 000 samples/s. All response waveforms within a 4 ms epoch (beginning at stimulus onset) were stored digitally for later analysis.

2.5. Data analysis

For this study, we focused on examining the gross-potential and single-fiber responses to cathodic stimuli. We did this for several reasons. First, cathodic stimuli evoke ECAP and single-fiber responses in the cat at lower stimulus levels than do anodic stimuli. Second, cathodic responses are apparently less prone to adaptation-like changes we have previously observed from both the ECAP and single fibers (Miller et al., 1998,

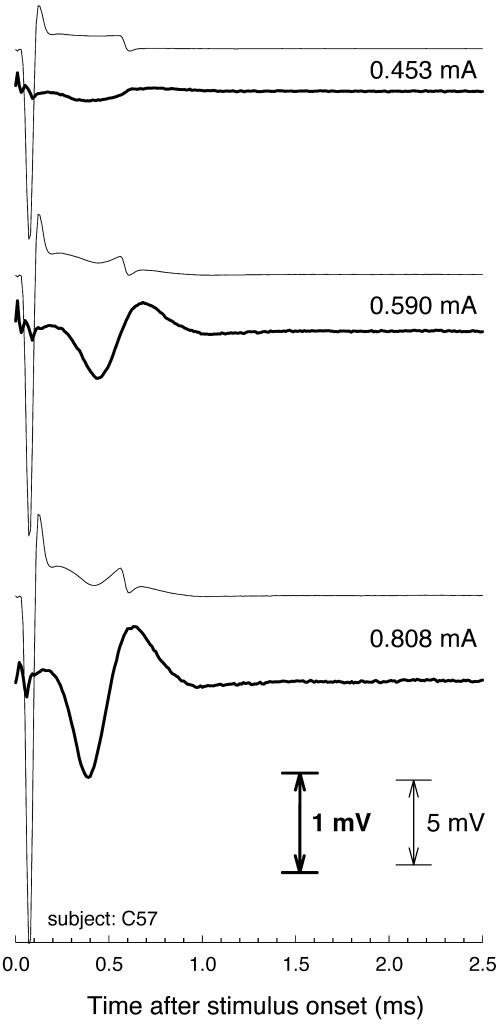

Fig. 2. Examples of ECAP response waveforms and demonstration of the use of a 'template' to reduce stimulus artifact contamination. Shown are three response waveforms obtained at different stimulus levels before (thin lines) and after (thick lines) application of the template scheme. In these cases, a biphasic stimulus with a second-phase duration of 500 μs was used. Different vertical scales were used to plot the pre- and post-template waveforms.

1999a). Finally, since cathodic stimuli produce ECAPs with longer latencies, the resultant waveforms are less prone to stimulus artifact contamination than are anodic responses. The data presented here may not be applicable to results obtained using anodic stimulation, since opposite-polarity stimuli likely depolarize fibers at different sites and in different spatial distributions.

Data were analyzed after the conclusion of each experiment using custom software. ECAP amplitude was defined as the voltage difference between the prominent negative N1 peak and the subsequent positive P2 peak (Miller et al., 1998). ECAP latency was measured from the onset of the recorded stimulus artifact to the P2 peak. This late peak was chosen to minimize the possibility of contamination of latency measures by the stimulus artifact. To reduce contamination of the ECAP waveform by stimulus artifact, we employed a template subtraction technique (Miller et al., 1998, 2000). Examples of this procedure are shown for three stimulus levels in Fig. 2, where 'raw' response waveforms are plotted with thin lines and the template-corrected waveforms are depicted with thick lines. In these examples, the second-phase duration was 500 μs, a particularly challenging duration since the second phase terminates in the midst of the ECAP response. As this example demonstrates, the template procedure can extract the ECAP response from the stimulus artifact with little distortion to the waveform.

ECAP threshold was defined as the stimulus level evoking a response amplitude 10% of that produced at the saturated (maximal) response. In a few cases (e.g. Fig. 3B), amplitude-level functions did not strictly reach saturation or a horizontal asymptote. In those instances, the 'knee' of the function (the point at which the slope underwent the largest decrement) was chosen as the saturation amplitude. Estimation of threshold typically involved interpolation of input–output functions. The slope of the ECAP amplitude-level function was computed on a piecewise (segment-by-segment) basis; maximum slope was the greatest value over all segments. Single-fiber threshold was defined as the level that produced a firing efficiency (FE) of 50%. Single-fiber latency was defined as the interval between stimulus onset and the peak of the action potential. Jitter was defined as the standard deviation of spike latencies. Mean latency and jitter were computed for the stimulus level yielding 50% FE. Threshold, mean latency, and jitter estimates usually required interpolation of the respective input–output function. Relative spread, or RS (Verveen, 1961) was computed by fitting FE vs. level data to an integrated Gaussian function to compute its standard deviation, which was done by linear regression to a probit transformation of the data. In doing so, we required a minimum of three points with FE values between 5 and 95%; on average, over six points were used for each RS estimate. Prior to the collection of single-fiber data, an ECAP amplitude-level function was obtained from each cat in order to assess each preparation's sensitivity to electrical stimulation.

Example ECAP amplitude-level functions from a cat and a guinea pig are shown in Fig. 3A,B. For both subjects, a total of 12 amplitude-level series were collected using different second-phase durations. Among the 12 series are replications of selected phase durations. These repeated conditions allowed us to assess the stability of each preparation over time, needed because data collection typically required 2–3 h. For subject C57 (Fig. 3A), the level of stability was high, as is evident from the three repeated series obtained with a

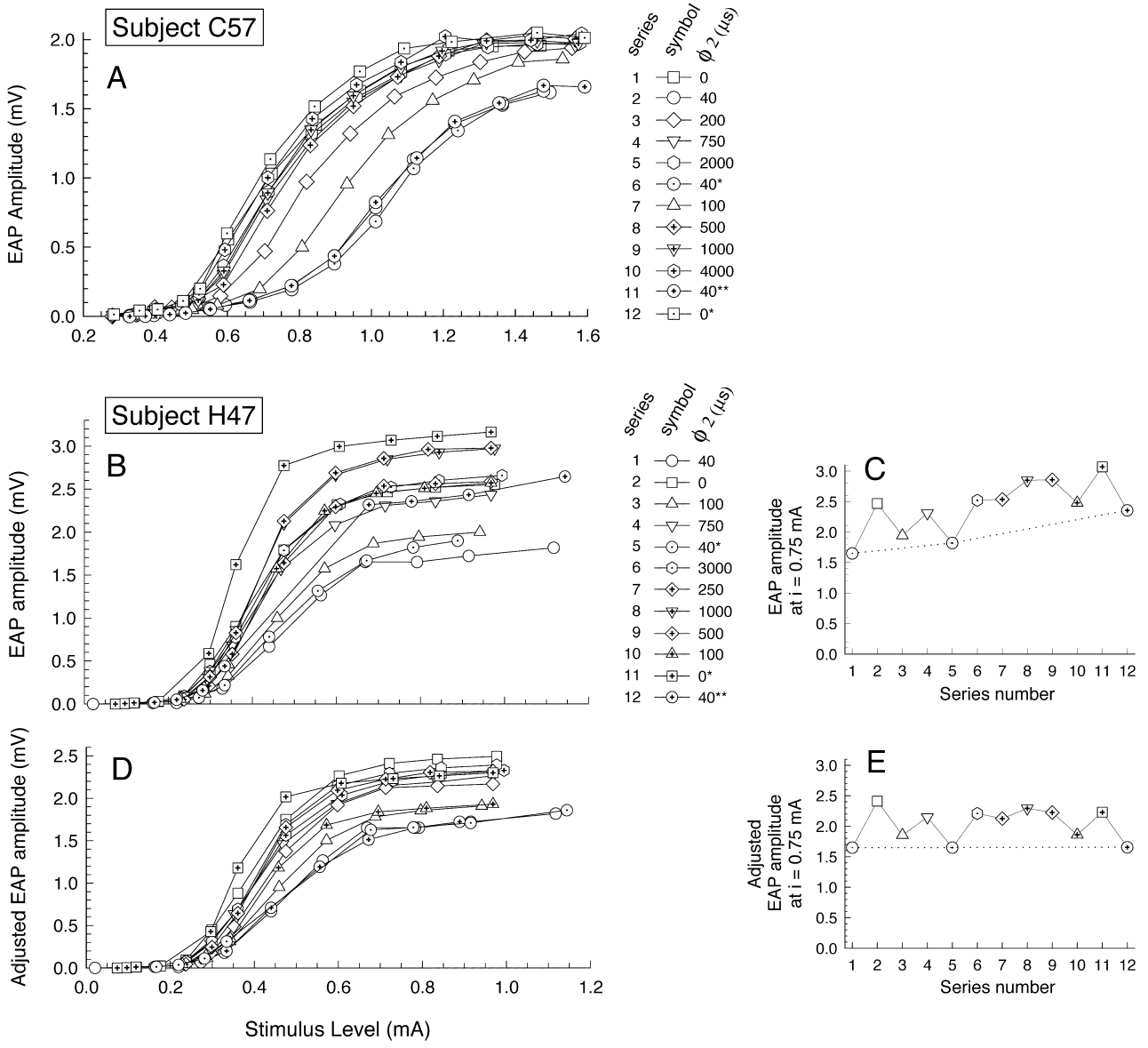

Fig. 3. ECAP amplitude-level data obtained from a cat (A) and a guinea pig (remaining panels) across 12 data sets. All stimulus pulses had a first-phase duration of 40 μs. The stimuli differed by the duration of the second (recovery) phase, as indicated by the legend. A second-phase duration of 0 indicates the monophasic condition. In the case of cat C57, the three repeated functions obtained with 40 μs/phase pulses (circular symbols) are nearly coincident. With guinea pig H47, however, significant drift in response amplitude is seen across data sets. This is shown explicitly in C, where ECAP amplitude at a fixed stimulus level is plotted for the 12 data sets. These data were used to compute drift correction factors for each amplitude-level function. Adjusted data are shown in D and E.

second-phase duration of 40 μs. The data of subject H47, however, demonstrate one of the least stable response amplitudes over the course of data collection. Saturation response amplitudes are plotted for each series in Fig. 3C, where an upward drift in ECAP amplitude is evident. The dotted line connects repeated measures and indicates the degree of drift over time. This pattern is typical of animal exhibiting drift in that, while response amplitude varied, preparation sensitivity (as determined by ECAP threshold) did not change appreciably. We attributed the shifts to changes in recording conditions such as brain or nerve tissue swelling in the vicinity of the recording electrode. To adjust for this drift, we applied correction factors to each amplitude-level function. These factors were defined using the data and dotted line in Fig. 3C by computing the ratio of the ECAP amplitude for series 1 and the amplitude predicted for each series by the dotted line. The results of these corrections are shown in Fig. 3D,E. Note that in Fig. 3E, less of the across-series

variance is simply due to a time effect. Corrections similar to these were applied in two other preparations where the drift across repeated conditions resulted in an amplitude change greater than 5%.

2.6. Computational modeling

To assist with interpretation of the physiological data, we include results using a computational model of the electrically stimulated nerve fiber. This model simulates the central axon of a feline auditory nerve fiber and incorporates the stochastic properties of each node of Ranvier. Details of this model are described in Rubinstein (1995). Briefly, the nerve fiber, based upon the anatomy of cat fibers, models 24 nodes of Ranvier and assumes a 2.5 μm fiber diameter. Each node consists of 4149 stochastic sodium channels and passive membrane properties (conductance and capacitance). The internodes were represented by nine passive elements. The stimulating electrode was modeled as a point-source positioned 500 μm above the fourth node of Ranvier, measured from the distal axon terminal. This position was deemed a reasonable approximation to a typical electrode-fiber orientation in our cat preparations, as we used a basally located stimulus electrode and assumed that the central axons of most fibers made the closest approach to the electrode. The modeled membrane potential was obtained at the 15th node of Ranvier, nine nodes from the proximal terminal. The kinetics of each voltage-sensitive sodium channel in each axon were simulated in 1 μs time steps. Calculations were performed in parallel on a cluster of three 500 MHz Macintosh G4s running the Message Passing Interface (http://exodus.physics.ucla.edu/appleseed/appleseed.html) under Absoft ProFortran 6.2 (http://www.absoft.com). Our previous algorithm for determining sodium channel open and close events was modified in favor of a more efficient approach (Mino et al., 2000; White et al., 2000). Code was partially optimized for the vector architecture of the G4 (Velocity Engine (Apple) or Altivec (Motorola)) eliminating the need for outside supercomputer resources.

3. Results

We collected data comparing the ECAPs obtained from cathodic 40 μs monophasic and cathodic-first 40 μs/phase biphasic pulses from 11 guinea pigs and 13 cats. ECAP amplitude-level and latency-level functions were analyzed to compare the responses to the two stimuli. We also collected ECAP data from a smaller set of subjects (four guinea pigs and three cats) in which the second-phase duration was systematically varied. Finally, we obtained analogous measures from 27 single fibers.

3.1. ECAP responses evoked with 40 μs monophasic and 40 μs/phase biphasic stimuli

ECAP responses were collected in response to 40 μs monophasic and 40 μs/phase biphasic pulses at several stimulus levels to characterize them over the entire dynamic range. To examine across-animal trends, we obtained the aforementioned ECAP amplitude and latency measures and compared the monophasic and biphasic data sets. In five of the 24 subjects, ECAP amplitude-level functions failed to demonstrate a flat, asymptotic, saturation region, but were instead characterized by an upward-sloping saturation. We attributed the problem in these cases to an unfavorably large stimulus artifact that was not effectively cancelled by our techniques. This problem usually affected the 40 μs/phase biphasic functions. In those cases, we omitted the estimates of saturation amplitude from group analyses.

3.1.1. ECAP amplitude and threshold measures

Fig. 4 provides across-animal comparisons of ECAP measures obtained with 40 μs monophasic and 40 μs/phase biphasic stimuli. Both guinea pig and cat data are shown. In each of the four panels, data from individual subjects are plotted with open symbols; mean values for each species are plotted with filled symbols. The mean value data are also summarized in Table 1. We used paired-comparison *t*-tests to evaluate the monophasic–

Table 1
Mean ECAP measures obtained from cats and guinea pigs

	Cat				Guinea pig			
	Monophasic	Biphasic	Difference	*n*	Monophasic	Biphasic	Difference	*n*
Threshold (mA)	0.473	0.697	−3.4 dB	13	0.288	0.350	−1.7 dB	11
Maximum amplitude (mV)	2.37	2.36	0.037 dB	9	1.97	1.71	1.2 dB	10
Maximum slope (mV/mA)	4.18	2.77	3.6 dB	13	6.31	4.56	2.8 dB	11
Maximum slope, normalized	3.30	3.31	−0.026 dB	13	2.70	2.27	1.51 dB	11
P2 latency at threshold (μs)	726	633	83 μs	13	658	591	67 μs	11
P2 latency at saturation (μs)	600	528	72 μs	13	592	519	73 μs	11

Monophasic data were obtained using 40 μs cathodic pulses and biphasic data were obtained using 40 μs/phase (cathodic-first) pulses. All stimuli were delivered by a monopolar intracochlear electrode. See also Figs. 4 and 5.

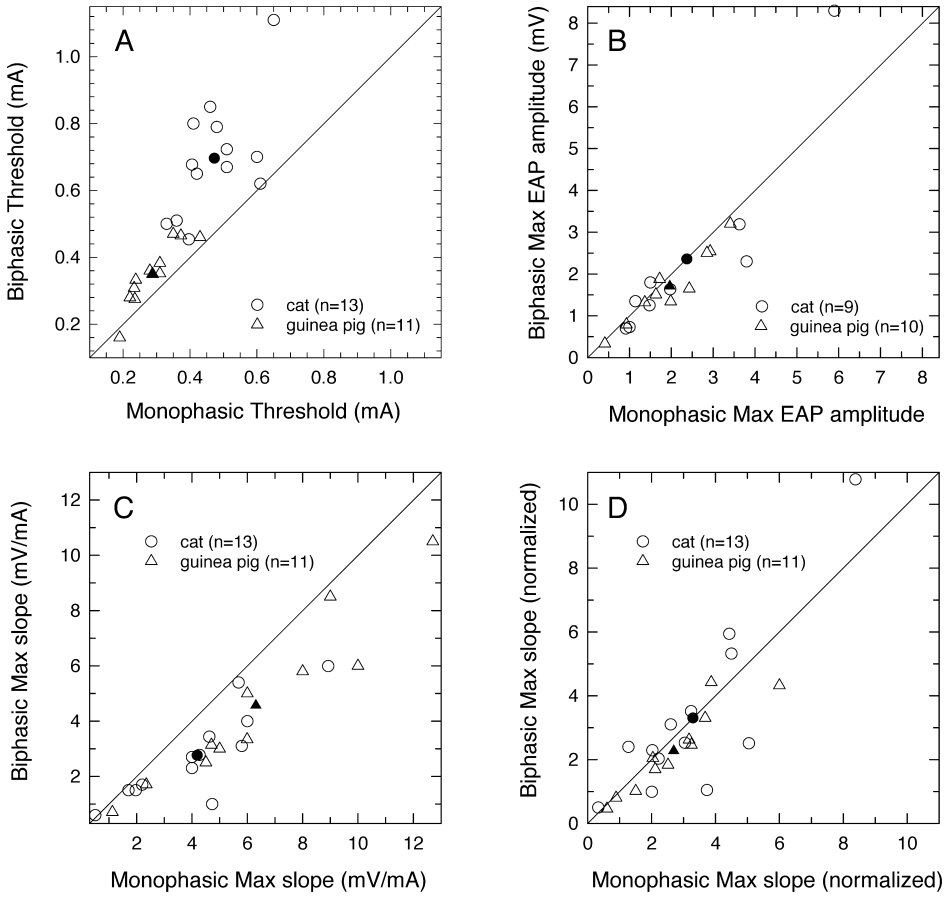

Fig. 4. Summary of ECAP measures obtained from 11 cats and 13 guinea pigs using both 40 μs monophasic and 40 μs/phase biphasic stimulus pulses. Mean values for cats and guinea pigs are plotted with filled symbols. Threshold (A) was defined as the stimulus level producing an amplitude 10% of the maximum amplitude. Maximum amplitude (B) was the ECAP amplitude obtained at a stimulus level sufficient to saturate the amplitude-level function. Maximum slope of each subject's amplitude-level function was computed in two different ways. It was first computed (C) as the maximum rate of increase over all the segments of each amplitude-level function. These values were then normalized (see text) to account for differences in thresholds across subjects (D).

biphasic differences for each species. These comparisons are discussed below and summarized in Table 2.

The data of Fig. 4A show a bias toward lower monophasic thresholds. In cats, the mean monophasic threshold was 3.4 dB lower than the mean biphasic threshold, while in guinea pigs, the mean monophasic threshold was 1.7 dB lower. These trends are statistically significant in both species (Table 2). Significant trends are also evident in the maximum slope of the ECAP amplitude-level functions (Fig. 4C), with monophasic stimuli producing greater slopes. However, because both threshold and maximum slope varied with the stimulus type, the slope measurement may be confounded by level effects. To address this, we computed normalized maximum slope values by multiplying each slope value by the stimulus level at which maximum slope occurred. In the case of the cat data, the normalized slopes failed to demonstrate a bias toward one stimulus type, as is seen graphically (Fig. 4D) and in the paired *t*-test (Table 2). In the guinea pig data, however, there is a small bias toward greater normalized slopes with monophasic stimuli. A paired-comparison *t*-test indicates a significant difference at a 3% probability of error. With regard to maximum (saturation) ECAP amplitude (Fig. 4B), the guinea pig data also demonstrated a small, but statistically significant bias toward greater amplitudes with monophasic stimuli. The cat saturation amplitudes did not demonstrate a significant bias, even with exclusion of the outlier point at the top of the plot.

3.1.2. ECAP latency measures

We also observed differences in the latency of the ECAP waveform in response to monophasic and biphasic stimuli. Fig. 5 provides comparisons of monophasic–biphasic effects observed in P2 latency for both species. P2 latency was assessed at both threshold stimulus level (Fig. 5A) and at a level required for a saturated response (Fig. 5B). Mean values of P2 latency at thresh-

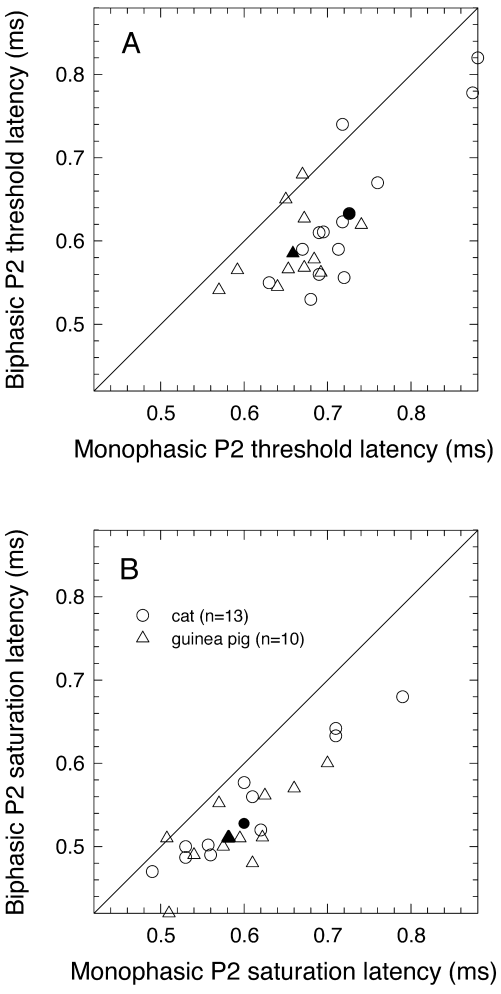

Fig. 5. Summary of ECAP latency measures obtained from 13 cat and 10 guinea pig preparations. The latency of the P2 peak (the positive peak occurring after the prominent negative peak) was measured from the onset of the stimulus pulse. A plots P2 latencies measured at threshold, i.e. at a response amplitude 10% of the maximum ECAP amplitude. B plots P2 latencies measured at the stimulus level at which ECAP amplitude was maximal. Mean values for each species are plotted using filled symbols.

old and saturation levels are listed in Table 1. In both measures and in both species, statistically significant effects are observed, with longer P2 latencies measured for monophasic stimuli than for biphasic stimuli (Table 2).

3.2. ECAP measures obtained with a range of second-phase durations

We obtained ECAP amplitude-level functions while systematically varying the second-phase duration in four guinea pig and three cat preparations. These functions were characterized by their threshold level as well as the ECAP amplitude obtained at a fixed stimulus level. For the latter measure, the stimulus level chosen was that which yielded an amplitude 50% of maximum when a 40 μs/phase biphasic stimulus was used. These threshold and amplitude data are shown in Fig. 6, plotted as a function of second-phase duration. While there were across-animal variations, some trends were evident in both data sets. Thresholds generally decreased with increasing second-phase duration, while ECAP amplitudes generally increased with second-phase duration. There was also an indication that these trends saturate with increasing phase duration: the greatest changes in threshold and amplitude occur for second-phase durations less than 500 μs. In Fig. 6, phase duration is plotted on a logarithmic axis; the saturation trend would be more evident on a linear plot.

3.3. Single-fiber measures

We collected 40 μs monophasic and 40 μs/phase biphasic input–output functions from 27 fibers of four cats. Fig. 7 summarizes how the threshold, mean latency, jitter, and relative spread differ for monophasic and biphasic stimuli. Individual single-fiber data are plotted in the figure by open circles and mean values by filled circles. These mean values and the mean monophasic–biphasic differences are listed in Table 3. Fig. 7A indicates that monophasic thresholds were typically lower than biphasic thresholds. On average, monophasic thresholds were 4.1 dB lower and a paired *t*-test

Table 2
Results of paired-comparison *t*-tests performed across the 40 μs monophasic and 40 μs/phase biphasic ECAP data sets of Table 1

	Cat			Guinea pig		
	t	*P*	d.f.	*t*	*P*	d.f.
Threshold (mA)	**−5.94**	**0.0003**	**12**	**−5.05**	**0.0005**	**10**
Maximum amplitude (mV)	0.0276	0.9790	8	**2.87**	**0.0184**	**9**
Maximum slope (mV/mA)	**4.34**	**0.0010**	**12**	**5.37**	**0.0003**	**10**
Maximum slope, normalized	−0.025	0.981	12	**2.51**	**0.0306**	**10**
P2 latency at threshold (ms)	**7.28**	**< 0.0001**	**12**	**4.43**	**0.0013**	**10**
P2 latency at saturation (ms)	**6.08**	**< 0.0001**	**12**	**6.21**	**< 0.0001**	**10**

Listed are the *t*-statistic (*t*), probability (*P*), and degrees of freedom (d.f.) for each test.

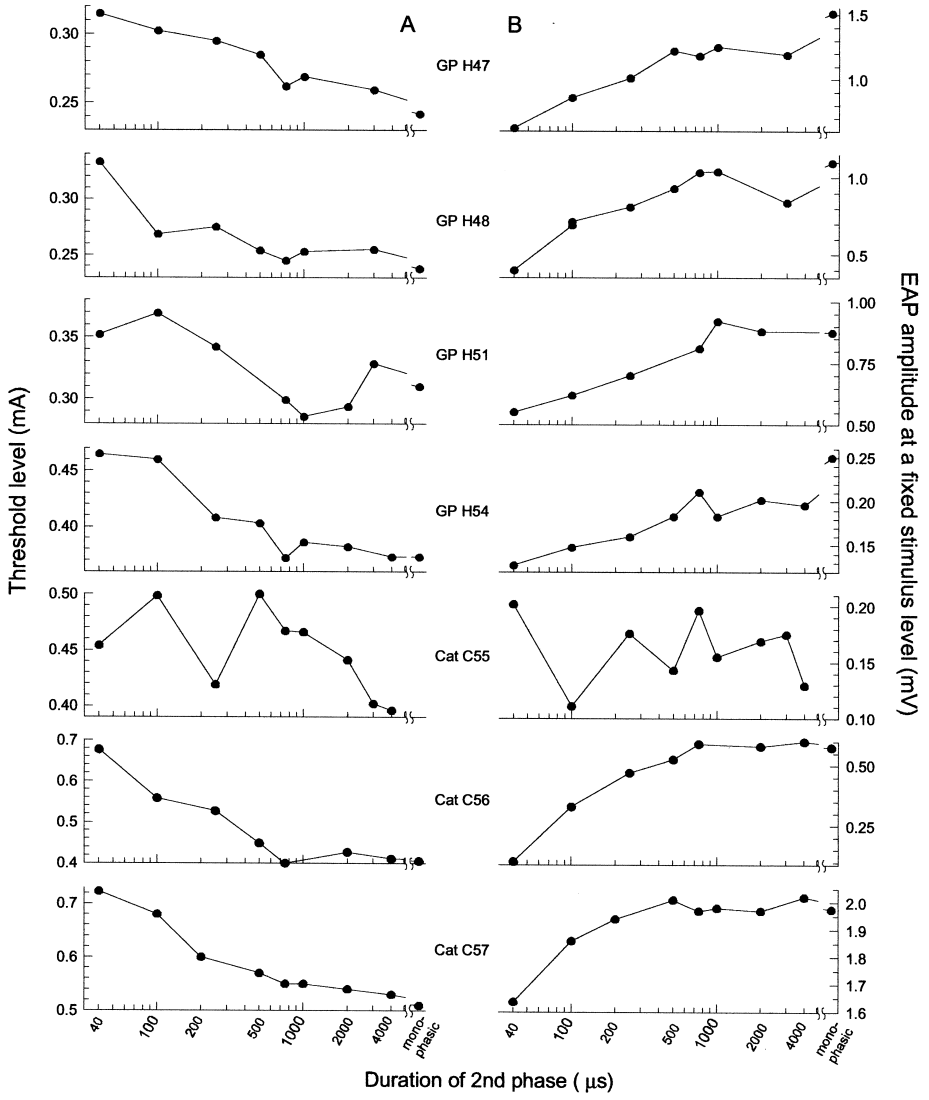

Fig. 6. The effect of the duration of the second stimulus phase on ECAP threshold level (column A) and ECAP amplitude at a fixed stimulus level (column B). Data are shown from all four guinea pig and three cat subjects from which such data were collected. For the data of column B, the stimulus level was chosen for each animal such that a 40 μs/phase biphasic pulse produced an ECAP amplitude one-half that of the maximum amplitude.

indicates that this difference is statistically significant (Table 4). A statistically significant trend was also observed in the analysis of mean spike latency. These data are plotted in Fig. 7B. On average, monophasic mean latency was 71 μs longer. Spike jitter was similar for both stimulus waveforms (Fig. 7C) and no statistical difference was observed. Finally, the relative spread data were slightly biased toward larger values for monophasic stimuli (Fig. 7D). A *t*-test over all the data did not indicate a significant trend; however, after

Table 3
Mean single-fiber measures obtained using 40 μs/phase monophasic and biphasic stimuli delivered by a monopolar intracochlear electrode

	Monophasic	Biphasic	Difference	*n*
Threshold (mA)	0.539	0.852	−0.312 (−4.06 dB)	27
Latency at 50% FE (μs)	588	517	71 μs	26
Jitter at 50% FE (μs)	83.2	85.5	−2.3 μs	27
Relative spread (%)	5.11	4.87	0.0019	25
Relative spread, outliers removed (%)	4.80	4.05	0.0074	22

Threshold, latency, and jitter were all defined for the condition of 50% FE. See also Fig. 7.

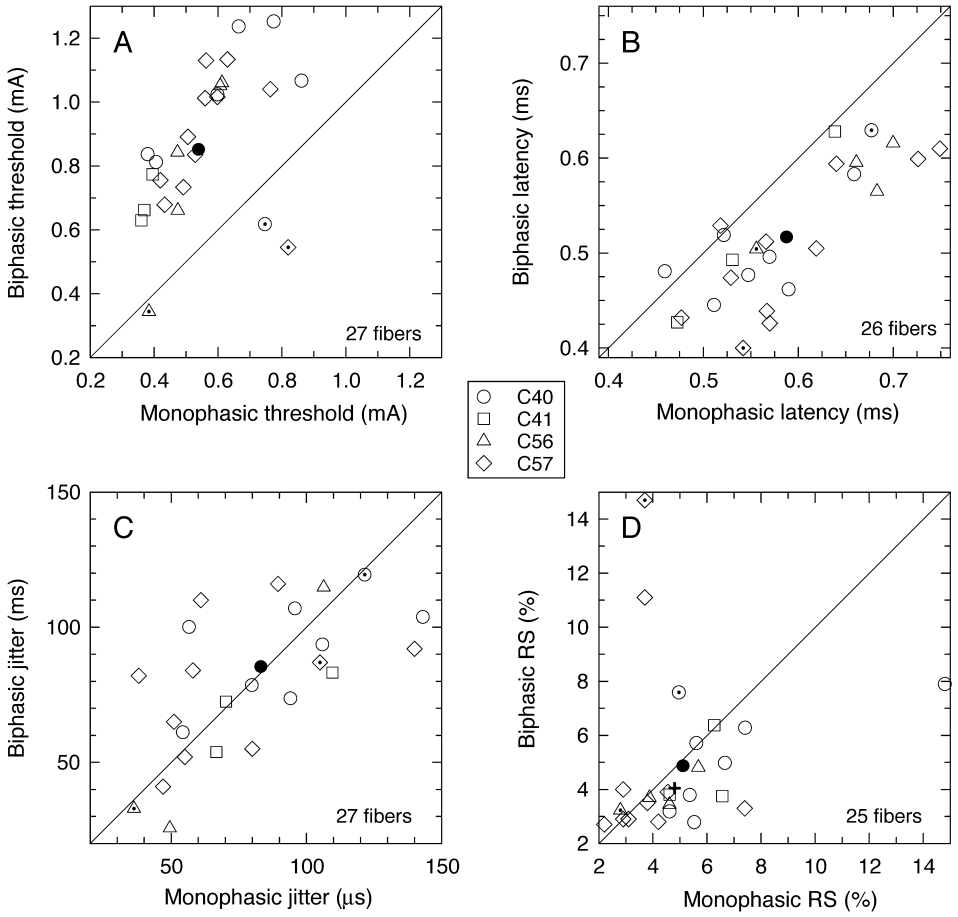

Fig. 7. Summary of four single-fiber measures obtained using both 40 μs/phase monophasic and biphasic stimuli. Data from 28 fibers of four cats are shown by open symbols; mean values are shown by the filled symbols. Threshold, latency, and jitter were all defined at a FE of 50%. The cross symbol in the graph of D indicates the mean value when the three fibers with RS > 10% are removed. Three outlier points (biphasic threshold < monophasic threshold) are plotted in each panel with dotted symbols.

removal of the three data with the highest RS values (i.e. greater than 10%), a significant trend of larger monophasic RS values was observed.

The threshold plot of Fig. 7A includes data from three fibers that appear to be outliers, since their monophasic thresholds were higher than their biphasic thresholds. Further analysis revealed that these fibers were indeed atypical. The data of these three fibers are denoted by dotted symbols in each of the four graphs of Fig. 7. Two of the three outliers had atypically high RS values (Fig. 7D) and two had lower thresholds to anodic monophasic stimuli than to cathodic monophasic stimuli. This is in contrast to the strong trend for cat fibers to have lower cathodic thresholds (Miller et al., 1999a). The third fiber was one of only two fibers observed to demonstrate bimodal post-stimulus–time histograms, again, a phenomenon that is atypical (Miller et al., 1999a).

We also obtained single-fiber measures while systematically varying second-phase duration in 12 fibers of two cats. Threshold vs. second-phase phase duration is plotted for these fibers in Fig. 8 using both logarithmic (Fig. 8A) and linear (Fig. 8B) axes. Most of the fibers demonstrated similar trends over the range of

Table 4
Results of paired-comparison *t*-tests performed across the 40 μs monophasic and biphasic single-fiber data sets of Table 3

	t	*P*	d.f.
Threshold (mA)	**8.16**	**< 0.0001**	**26**
Latency at 50% FE (ms)	**7.55**	**< 0.0001**	**25**
Jitter at 50% FE (μs)	0.633	0.532	26
Relative spread (%)	0.275	0.785	24
Relative spread, outliers removed (%)	**2.41**	**0.0250**	**21**

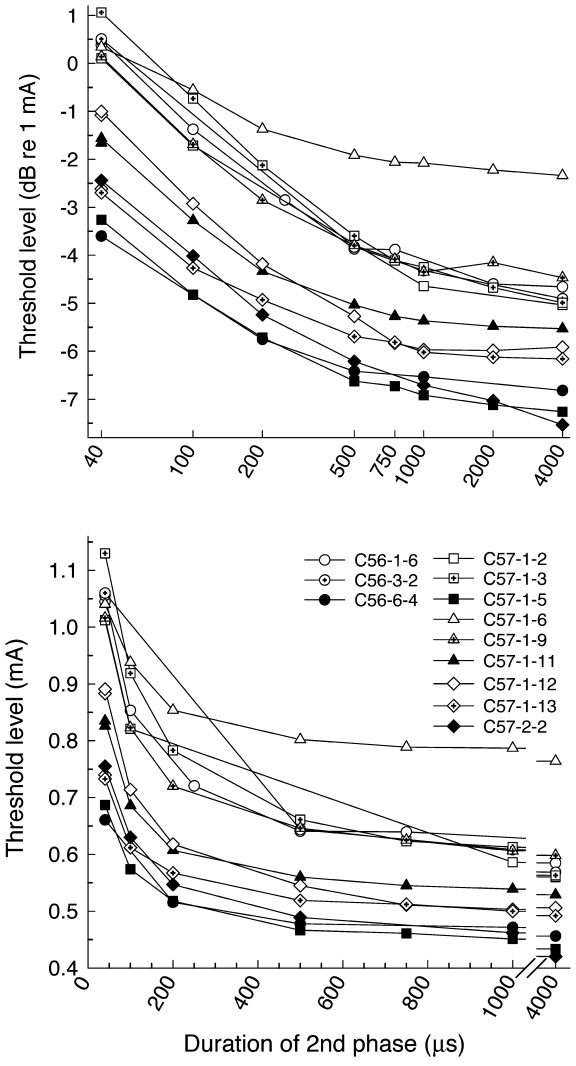

Fig. 8. The effect of systematic variation of the second-phase duration on single-fiber threshold. Shown are data from 12 fibers of two cats. Data are plotted using logarithmic (A) and linear (B) axes.

phase durations. Most decreased monotonically and reached asymptotic values at about 2 ms. Functions from the fibers generally decreased at comparable rates. The largest decreases in threshold occurred for second-phase durations of 500 μs or less.

3.4. Comparison of ECAP and single-fiber data

Comparisons of cat gross-potential and single-fiber measures made using data for the 40 μs/phase monophasic and biphasic stimulus conditions demonstrated two similarities. Mean threshold differences between monophasic and biphasic conditions were comparable for the single-fibers (4.1 dB) and ECAP (3.4 dB), as were threshold latency differences (single-fiber: 71 μs, ECAP: 83 μs). In both measures, *t*-tests of the single-fiber versus ECAP differences failed to reach significance at an error probability of 10%. We also examined whether monophasic–biphasic differences in the normalized cat ECAP slopes were significantly different than differences observed in single-fiber RS values. No significant differences (at a 10% probability of error) were found between the slope and RS measures, even after removal of the data from three fibers with unusually large RS values.

Single-fiber vs. ECAP comparisons can also be made with the systematic investigation of the effect of second-phase duration on threshold. In Fig. 9, the data of Figs. 6 and 8 are replotted, limiting the data to the two cats (C56 and 57) that yielded both single-fiber and ECAP measures. Threshold data for each fiber and ECAP data set are normalized to each set's threshold for the 40 μs/phase biphasic stimulus. The single-fiber and ECAP data demonstrate comparable ranges of second-phase durations over which threshold changes are evident. While the magnitude of the threshold decrements was comparable for both measures for subject C56, the ECAP function of subject C57 followed a shallower course. This disparity should be viewed cautiously, since the earlier comparison of 40 μs/phase monophasic–biphasic thresholds, which involved larger data sets, indicated similar magnitudes of effect for the single-fiber and ECAP data sets.

3.5. Interspecies comparison

Finally, we note both similarities and differences in

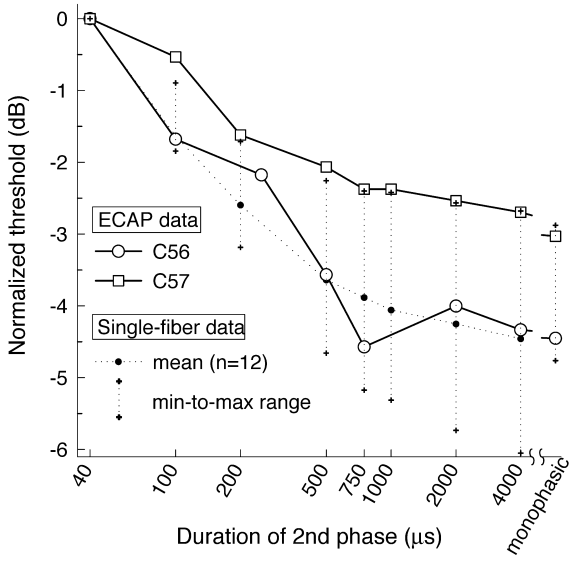

Fig. 9. A comparison of the effects of second-phase duration on ECAP and single-fiber thresholds. ECAP data from two cats are plotted using open symbols. Mean thresholds of 12 fibers from these two cats are also plotted (dotted line), along with vertical bars representing the minimum and maximum values. The data are the same as those plotted in Figs. 6 and 8, except that thresholds are normalized to the value obtained with a 40 μs/phase biphasic pulse.

the way that cats and guinea pigs respond to monophasic and biphasic current pulses. Both species demonstrated lower thresholds with 40 μs monophasic pulses than with 40 μs/phase biphasic stimuli. Response latencies were also longer in both species for monophasic stimuli. However, of the four ECAP measures assessed, we observed that the mean monophasic vs. biphasic threshold difference in cats (3.4 dB) was greater than the mean difference in guinea pigs (1.7 dB). An unpaired *t*-test comparing the threshold differences in cats and guinea pigs indicated that this difference is statistically significant ($t = 2.81$, $P = 0.010$, d.f. = 22). None of the other monophasic–biphasic differences listed in Table 1 was significantly different across the two species using an error probability of 10%.

3.6. Modeling results

We applied our computational neuron model to clarify differences observed between our single-fiber data and those of Shepherd and Javel (1999). Specifically, our single-fiber data revealed a monophasic vs. biphasic threshold advantage of about 4.1 dB while Shepherd and Javel reported a smaller (1.2 dB) advantage when investigating 100 μs/phase pulses. The model allowed us to test our hypothesis that such differences are due to the different first-phase durations used in the two studies. The model neuron was excited with cathodic-first biphasic and cathodic monophasic pulses of various phase durations. In one experiment, the model was stimulated with biphasic pulses with a first-phase duration of 100 μs and a systematically varied second-phase duration. The model was also stimulated with biphasic pulses with the first-phase duration held constant at 40 μs and the second phase systematically varied.

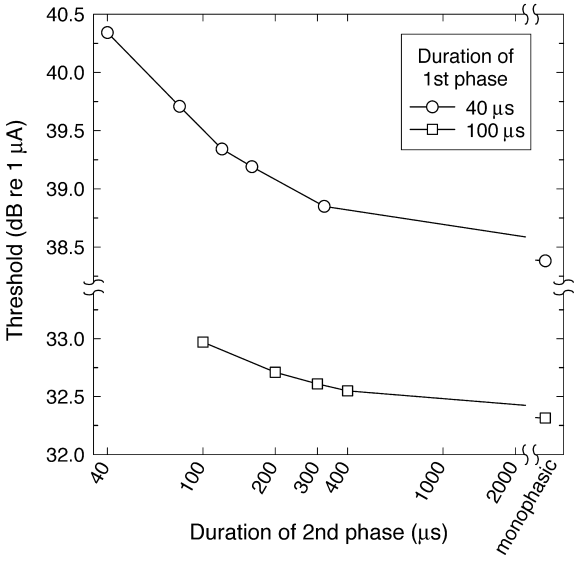

Fig. 10. Results of computational simulations of a single feline auditory nerve fiber. Single-fiber thresholds are plotted as a function of the second-phase duration of a charge-balanced biphasic pulse. Curves are shown for pulses with two different first-phase durations: 40 μs (circles) and 100 μs (squares).

In Fig. 10, model fiber thresholds are plotted as a function of second-phase duration for both the 40 μs/phase and 100 μs/phase stimuli. In both cases, threshold decreases monotonically as second-phase duration is increased. With a first-phase duration of 40 μs, monophasic threshold was found to be 2.0 dB lower than the biphasic threshold (Fig. 10, circles). Also, monophasic mean latency was 51 μs greater than that obtained with biphasic stimuli. While the absolute magnitudes of these trends differ from the experimental cat data, we note that the direction of each monophasic–biphasic difference observed with the model, as well as its relative significance, was consistent with the feline data. The model data of Fig. 10 also demonstrate the interaction of the duration of the first and second phases of biphasic pulses. While a 2.0 dB monophasic–biphasic threshold difference was observed with pulses having a first-phase duration of 40 μs, a smaller threshold difference (0.66 dB) was observed when manipulating biphasic pulses with a first-phase duration of 100 μs. This model result is instructive for comparing the single-fiber results obtained in this study and that of Shepherd and Javel (1999). The data indicate that a smaller monophasic–biphasic threshold difference is obtained with stimulus pulses having a larger first-phase duration. This is consistent with the smaller mean threshold difference reported by Shepherd and Javel (1999) with their 100 μs/phase stimuli.

The computational model also allowed us to survey the membrane voltage at each node of Ranvier to monitor the site of action potential initiation under different stimulus conditions. We observed that for both monophasic and biphasic stimuli, the initiation site was the node closest to the stimulating electrode. That is, the site of initiation was independent of the choice of monophasic or biphasic stimuli. Shepherd and Javel (1999) used bipolar intracochlear electrodes while our study employed a monopolar electrode. The excitation fields produced by these two arrangements are likely quite different and may have contributed to differences in the two data sets.

4. Discussion

This study examined single-fiber and gross-potential responses to monophasic, pseudomonophasic, and symmetric biphasic stimulus pulses in guinea pig and cat preparations. We focused on the responses to cathodic monophasic pulses and biphasic pulses with a cathodic-leading phase. Anodic stimuli likely produce different

membrane depolarization profiles; therefore, our results may not be applicable to anodic-first stimuli. In both species, significant differences in auditory nerve responses were observed with monophasic and biphasic current pulses. Compared with 40 μs/phase biphasic pulses, monophasic pulses produced lower thresholds and longer response latencies. Both trends are consistent with a simple interpretation of the excitable nerve fiber as a leaky current integrator coupled with a delay element. The resistive and capacitive membrane properties serve to integrate stimulus current, while the voltage-gated ionic channels introduce a time delay (e.g. Kandel et al., 2000). The combination of an integrator and delay element was discussed by van den Honert and Mortimer (1979) in their account of responses from frog sciatic nerves and qualitatively explains why a 40 μs monophasic pulse can excite a fiber while a 40 μs/phase biphasic pulse of the same amplitude fails to do so. While the first phase of the biphasic pulse may be of sufficient level to reach threshold, the delay in channel activation may facilitate the deactivation of the excitation process by the second phase. Thus, higher biphasic stimulus levels are needed for action potential initiation. This higher level, together with the fact that excitation is due to the first (cathodic) phase, results in the relatively shorter response latencies obtained with biphasic pulses. The fact that comparable differences in monophasic–biphasic threshold and latency were observed at the single-fiber and gross-potential levels strengthens our conjecture that the stimulus effects occur at the neural membranes of the auditory nerve.

Depending upon the method of data presentation, the slope of the ECAP amplitude-level function also varies with second-phase duration. As seen in Fig. 4C, slopes were greater with monophasic stimuli. However, when slopes were normalized by threshold (Fig. 4D), mean monophasic and biphasic slopes were virtually identical for cats and only a small bias toward greater monophasic slopes was evident in the guinea pig data. The single-fiber data were consistent with these results in that relative spread values were comparable for 40 μs/phase monophasic and biphasic stimuli. The RS measure uses a normalized stimulus level scale; thus, if stimulus level is incremented in constant-size current steps, monophasic stimuli will recruit fibers over a small range of current levels relative to the range for biphasic stimuli. However, if stimulus level is incremented in logarithmic steps, both monophasic and biphasic current pulses will recruit fibers over comparable ranges of stimulus levels. This finding is relevant to how cochlear implant devices encode stimulus level, since they are typically programmed to use logarithmic current steps. Relative spread was found to vary significantly with second-phase duration when fibers with large 'outlier' RS values were removed from the group analysis. However, even after removal of outliers, the magnitude of the difference in RS across monophasic and biphasic stimulus conditions was relatively small. Given previous studies of how RS influences modeled ECAP responses, it is not likely that this difference would measurably change the ECAP or the aggregate spike output of the auditory nerve (Miller et al., 1999b).

In addition to relative spread, the single-fiber measure of jitter had comparable values for 40 μs/phase monophasic and biphasic stimuli. Our observations that neither RS nor jitter comparisons demonstrated large differences and that differences in threshold and latency followed the behavior of a leaky integrator argue against the notion that the monophasic and biphasic stimuli excited neural membranes in fundamentally different ways. We conclude that it seems likely that both stimulus types excite equivalent sites on the neural membrane. Note also that our computational model results are consistent with this notion: the modeled site (node) of excitation was not found to change as the duration of the second phase was varied.

The main goal of this study was to determine how manipulation of a charge-balanced, two-phase stimulus waveform could increase excitation efficiency over that of symmetric biphasic pulses. Both the ECAP and single-fiber data indicate that, with a first-phase duration of 40 μs, relatively large threshold reductions are obtained as the second-phase duration is increased beyond 40 μs. The largest effects of the second phase are observed for second-phase durations less than 500 μs. For greater durations, asymptotically smaller incremental changes are observed. Thus, if a design goal for a cochlear prosthesis is to use 'pseudomonophasic' stimuli to effect threshold improvements, the data collected here suggest that relatively large threshold improvements can be realized by increasing second-phase duration up to 500 μs. This assertion may only be valid for biphasic stimuli with first-phase durations of 40 μs. Since neural membranes act as leaky integrators, one would expect smaller monophasic–biphasic threshold differences for longer first-phase durations. Our modeling data demonstrate this trend and likely explain why Shepherd and Javel (1999) found a relatively small (1.2 dB) improvement in single-fiber thresholds with 100 μs/phase monophasic pulses.

Although the selection of relatively long second-phase durations provides greater improvement in stimulus efficiency, design constraints relevant to multi-electrode stimulation strategies require consideration. The continuous interleaved strategy (CIS) used in many multi-channel cochlear implants is premised upon non-simultaneous stimulation of adjacent electrodes. Given the trend toward faster pulse rates, the total time available for charge recovery by a second, prolonged, phase is limited. However, it is not yet known

to what degree low-level (sub-threshold) currents on adjacent electrodes, such as those that might occur for charge recovery, may indeed cause unwanted interactions. Alternate methods of distributing a 'second phase' for charge recovery could be proposed. For example, a single rectangular recovery pulse could be replaced by a series of shorter-duration pulses that could be temporally distributed to preserve non-simultaneity. Alternatively, the second, recovery phase of a biphasic pulse could simply be delayed relative to the offset of the first phase. Due to the integrative and time-delay properties of fibers, such a delay would effectively reduce threshold, as has been demonstrated in the frog sciatic nerve (van den Honert and Mortimer, 1979) and cat auditory nerve (Shepherd and Javel, 1999). Such a technique can be employed in the Nucleus® device stimulation strategy, where interphase delay can be manipulated. Specific delays could be chosen in order to maintain the timing requirements of CIS stimulation. It should be kept in mind, however, that the use of a relatively long second phase (or a temporally distributed series of charge-recovery pulses) has an inherent advantage over the interphase delay approach. Since a longer second phase will be of reduced amplitude (and effective 'strength'), it is less likely to excite other neurons and therefore more likely to provide more selective excitation of neural elements.

Our observation that asymmetric biphasic pulses produced lower thresholds than symmetric biphasic pulses agrees with the single-fiber results of Shepherd and Javel (1999). In both studies, the level of the initial phase of the stimulus was greater than that of the recovery phase. However, in their psychophysical study, Coste and Pfingst (1996) found no threshold improvement with triphasic stimuli when compared to biphasic pulses. Their triphasic stimulus was composed of initial and final phases that flanked a center phase of opposite polarity that was twice the amplitude of the flanking phases. Taken together, these results suggest that the first phase of pseudomonophasic stimuli must be of smaller duration (and greater amplitude) than the subsequent phase in order to achieve a threshold improvement over symmetric biphasic waveforms.

Finally, we found a significant interspecies difference in the magnitude of the biphasic/monophasic threshold ratios, with cats demonstrating a larger ratio than guinea pigs. We previously reported that the guinea pig ECAP has a lower threshold to anodic stimuli than it does to cathodic stimuli, while the cat ECAP demonstrates the opposite trend (Miller et al., 1998). The lower anodic thresholds and smaller biphasic/monophasic threshold ratio observed in guinea pigs are likely interrelated. These interspecies differences may be due to gross differences in cochlear anatomy. In a uniform conducting medium, an axon with a monopolar electrode positioned over it will be more sensitive to cathodic stimuli than anodic stimuli (Rattay, 1986). The cathodic/anodic threshold ratios observed in cats are qualitatively consistent with the rather simple model predictions provided by Rattay's single-fiber 'activating function' construct. However, greater sensitivity to anodic stimuli observed in guinea pigs clearly requires a more sophisticated analysis of the membrane depolarization profiles that presumably occur in that species. We have no reason to assume that guinea pig fibers have markedly different response properties than cat fibers and therefore suspect that the spatial orientation of the fibers and the excitation fields created by the extraneural conditions play a role in the enhanced sensitivity to anodic stimuli in the guinea pig. Interspecies differences in spatial orientation and excitation fields may arise from the differing shapes of the helical spirals of the cat and guinea pig cochleae, as well as differences in the shape and radius of the lower turn and hook region of the two species. Thus, although we believe that the phase duration effects evident in both our single-fiber and ECAP data largely reflect conditions at the neural membrane, it is plausible that cochlear geometry also plays an important role. The complex pattern and orientation of fibers inherent in the cochlea may also account for the anomalous single-fiber data evident in Fig. 7.

5. Summary

We performed a systematic analysis of the effectiveness of asymmetric biphasic current pulses as alternatives to the symmetric biphasic pulses used in many cochlear prostheses. Asymmetric, cathodic-first, biphasic pulses evoked responses from the auditory nerves of cats and guinea pigs at levels lower than those needed for symmetric, cathodic-first, biphasic pulses. The degree of threshold improvement was dependent on the duration of the second (recovery) phase of the stimulus; progressively smaller improvements were seen as the second-phase duration was increased beyond about 500 μs. These improvements were observed in both the single-fiber and gross-potential responses. The degree of the effect was species-dependent, presumably due to anatomical differences between the guinea pig and cat cochleae. These results are relevant to the design of efficient functional electrical stimulation of excitable tissue.

Acknowledgements

We thank Dr. Hiroyuki Mino for implementing the improved algorithm for the computational model. We

also thank Ms. Diane M. Prieskorn, who shared her surgical expertise for deafening guinea pigs. Funding was provided by the NIH Neural Prosthesis Program (Contract N01-DC-9-2107) and the Iowa Lions Club.

References

Abbas, P.J., Brown, C.J., 1991. Electrically evoked auditory brainstem response: refractory properties and strength–duration functions. Hear. Res. 51, 139–148.

Bostock, H., 1983. The strength–duration relationship for excitation of myelineated nerve: computed dependency on membrane parameters. J. Physiol. (Lond.) 341, 59–74.

Brummer, S.B., Robblee, L.S., Hambrecht, F.T., 1983. Criteria for selecting electrodes for electrical stimulation: theoretical and practical considerations. Ann. N.Y. Acad. Sci. 405, 159–171.

Coste, R.L., Pfingst, B.E., 1996. Stimulus features affecting psychophysical detection thresholds for electrical stimulation of the cochlea. III. Pulse polarity. J. Acoust. Soc. Am. 99, 3099–3108.

Frijns, J.H.M., de Snoo, S.L., ten Kate, J.H., 1996. Spatial selectivity in a rotationally symmetric model of the electrically stimulated cochlea. Hear. Res. 95, 33–48.

Kandel, E.R., Schwartz, J.H., Jessell, T.M., 2000. Principles of Neural Science, 3rd edn. Elsevier Science, New York.

McIntyre, C.C., Grill, W.M., 2000. Selective microstimulation of central nervous system neurons. Ann. Biomed. Eng. 28, 219–233.

Miller, C.A., Woodruff, K.E., Pfingst, B.E., 1995. Functional responses from guinea pigs with cochlear implants. I. Electrophysiological and psychophysical measures. Hear. Res. 92, 85–99.

Miller, C.A., Abbas, P.J., Rubinstein, J.T., Robinson, B.K., Matsuoka, A.J., Woodworth, G., 1998. Electrically evoked compound action potentials of guinea pig and cat: responses to monopolar, monophasic stimulation. Hear. Res. 119, 142–154.

Miller, C.A., Abbas, P.J., Robinson, B.K., Rubinstein, J.T., Matsuoka, A.J., 1999a. Electrically evoked single-fiber action potentials from cat: responses to monopolar, monophasic stimulation. Hear. Res. 130, 197–218.

Miller, C.A., Abbas, P.J., Rubinstein, J.T., 1999b. An empirically based model of the electrically evoked compound action potential. Hear. Res. 135, 1–18.

Miller, C.A., Abbas, P.J., Brown, C.J., 2000. An improved method of reducing stimulus artifact in the electrically evoked whole nerve potential. Ear Hear. 21, 280–290.

Mino, H., Rubinstein, J.T., Miller C.A., Abbas, P.J., 2000. Effects of remaining hair cells on cochlear implant function. 4th Quarterly Progress Report, N01-DC-9-2106.

Pfingst, B.E., DeHann, D.R., Holloway, L.A., 1991. Stimulus features affecting psychophysical detection thresholds for electrical stimulation of the cochlea. I. Phase duration and stimulus duration. J. Acoust. Soc. Am. 90, 1857–1866.

Rattay, F., 1986. Analysis of models for external stimulation of axons. IEEE Trans. Biomed. Eng. 33, 974–977.

Rubinstein, J.T., 1995. Threshold fluctuations in an N sodium channel model of the node of Ranvier. Biophys. J. 68, 779–785.

Shepherd, R.K., Javel, E., 1999. Electrical stimulation of the auditory nerve: II. Effect of stimulus waveshape on single fibre response properties. Hear. Res. 130, 171–188.

van den Honert, C., Mortimer, J.T., 1979. The response of the myelinated nerve fiber to short duration biphasic stimulating currents. Ann. Biomed. Eng. 7, 117–125.

van den Honert, C., Stypulkowski, P.H., 1984. Physiological properties of the electrically stimulated auditory nerve. II. Single fiber recordings. Hear. Res. 14, 225–243.

Verveen, A.A., 1961. Fluctuation in Excitability. Drukkerij, Holland N.V., Amsterdam.

West, B.A., Brummett, R.E., Himes, D.L., 1973. Interaction of kanamycin and ethacrynic acid. Arch. Otolaryngol. 98, 32–37.

White, J.A., Rubinstein, J.T., Kay, A.R., 2000. Channel noise in neurons. Trends Neurosci. 23, 131–137.

Xu, S.A., Shepherd, R.K., Chen, Y., Clark, G.M., 1993. Profound hearing loss in the cat following the single co-administration of kanamycin and ethacrynic acid. Hear. Res. 70, 205–215.